J Mater Sci (2010) 45:4578–4582
DOI 10.1007/s10853-010-4381-z

ULTRAFINE GRAINED MATERIALS

Continuous high-pressure torsion

Kaveh Edalati · Zenji Horita

Received: 10 February 2010 / Accepted: 3 March 2010 / Published online: 16 March 2010

Abstract Continuous high-pressure torsion (CHPT) was developed as an expeditious process to effect severe plastic deformation. Using the CHPT, sheets of high purity aluminum, copper, and iron were successfully processed by introducing intense shear strain under high pressure. The results of hardness measurements after CHPT were well consistent with those of CHPT using disk and ring specimens. Microstructural observations demonstrated that CHPT can be used as a continuous process for grain refinement.

Introduction

Significant grain refinement is achieved by processing metallic materials through the application of severe plastic deformation (SPD) [1]. Several methods were developed for the SPD process, which mainly include equal-channel angular pressing (ECAP), high-pressure torsion (HPT), accumulative roll-bonding (ARB), multi-directional forging (MDF), cyclic extrusion and compression (CEC) and repetitive corrugation and strengthening (RCS) [2]. Among different techniques for the SPD process, HPT is especially effective to introduce extremely large shear strains for the grain refinement. Because the HPT is operated under high hydrostatic pressures, the fracture is significantly suppressed, and thus it is applicable to hard and less ductile materials such as molybdenum [3], tungsten [4], and intermetallics [5]. In the HPT method which was first invented by Bridgman in 1935 [6], a small thin disk is placed between two massive anvils under a high pressure and intense shear strain is introduced by rotating the two anvils with respect to each other.

The HPT process has three main limitations: first, the sample shape is in the form of disk which is not suitable for many industrial applications when compared to wire or sheet forms; second, the sample size is generally limited to a maximum of 35 mm in diameter to maintain a high degree of applied pressure; third, because the strain is generated in proportion to the distance from the disk center, an inhomogeneous distribution of microstructure is developed across the diameter. In order to overcome these limitations, the HPT using ring shape, which is more appropriate than disk shape for industrial application, was introduced [7] with a simple modification of the earlier design [8, 9]. Using the ring HPT, it is possible not only to eliminate a less-strained and coarse-grained center part [7, 10, 11] but also to scale up the sample, for example, to 100 mm in diameter [12]. As another attempt to improve the sample shape, the high-pressure sliding (HPS) was developed for producing sheet metallic materials with 5-mm width, 0.8-mm thickness and 100-mm length [13]. In both ring HPT and HPS, the sample size is still limited because the pressure is sacrificed with any increase in the sample size. For example, in order to process with HPT for disk with 500-mm diameter under a pressure of 2 GPa, the compression load should be 39,000 tons. In order to process with HPT for a ring with 500 mm in outer diameter and 3 mm in width under a pressure of 2 GPa, the compression load should be 940 tons. For HPS processing of a sheet with 500-mm length and 5-mm width under a pressure of 2 GPa, the compression load should be 500 tons.

In this study, therefore, a new alternative SPD process is developed for processing of metallic sheets with HPT in a continuous manner, which we call continuous high-

K. Edalati (✉) · Z. Horita
Department of Materials Science and Engineering, Faculty of Engineering, Kyushu University, Fukuoka 819-0395, Japan
e-mail: kaveh.edalati@zaiko6.zaiko.kyushu-u.ac.jp

pressure torsion (CHPT). Using the CHPT, the sample is processed in an expeditious way so that the sample size is increased without sacrificing the pressure.

Experimental materials and procedures

The facility for the CHPT, as schematically illustrated in Fig. 1, consists of two anvils: the lower anvil, which is rotated during process, has a flat surface with a roughened ring-shaped area; and the upper anvil, which is fixed during process, has a half ring-shaped groove on the surfaces with 0.5-mm depth, 3-mm width, and and outer diameter (*OD*) of 20 or 30 mm. The surface roughness of the upper anvil is reduced with respect to the surface roughness of the lower anvil to induce a continuous flow of the material due to the difference in slippage. A U-shaped specimen with 1-mm thickness, as shown in Fig. 1, is used as an initial sample. Each sample is placed on the lower anvil, and the pressure is applied on the sample by raising the lower anvil up to a make rigid contact with the upper anvil. The lower anvil is then rotated with respect to the upper anvil, and shear strain is introduced in the sample under a high pressure. Accordingly, the material starts to flow in the direction of rotation. Figure 2 shows the appearance of a Cu sample with $OD = 20$ mm, before and after CHPT.

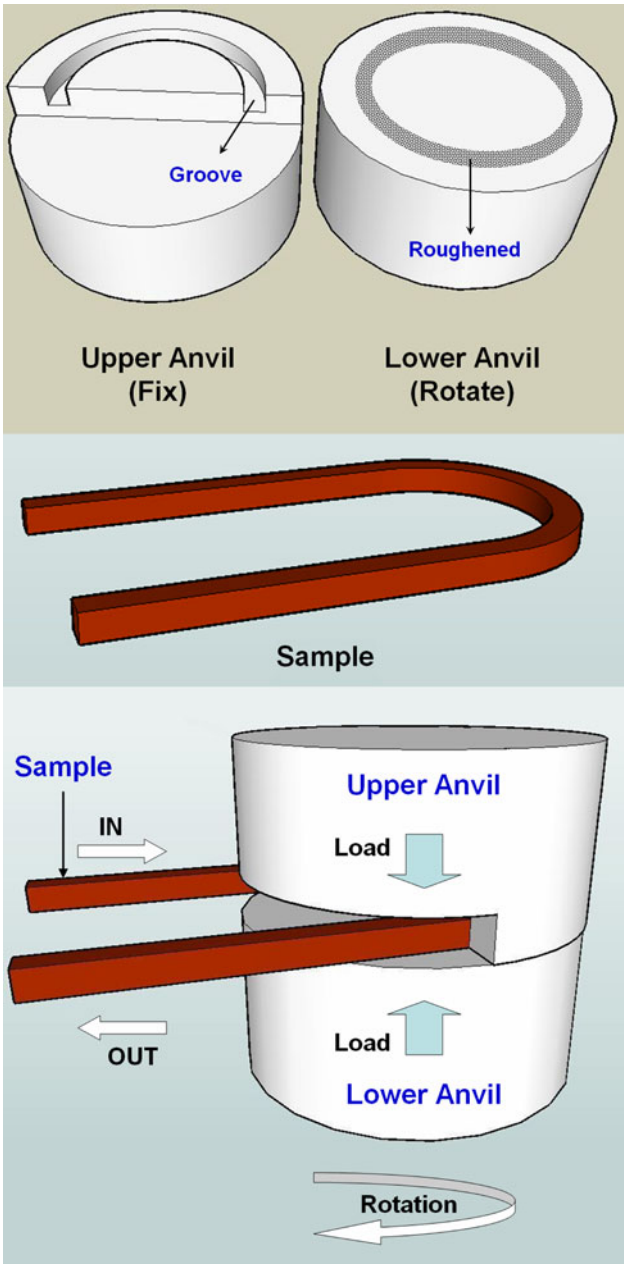

Fig. 1 Schematic illustration of CHPT

The equivalent strain produced by CHPT, ε, is calculated as follows:

$$\varepsilon = (1 - s)\frac{\pi R}{\sqrt{3}t} \quad (1)$$

where s is the fraction of sample slippage, R is the mean radius of U-shaped sample, as shown in Fig. 2, and t is the thickness of sample. For this study, R was either 8.5 or 13.5 mm, and t was 0.6 mm. The slippage was evaluated, as described in detail in an earlier article [14], by measuring the discrepancy of the markers made on both surfaces of the sample after rotating by a quarter revolution (90°). It turned out that the slippage was negligibly small for the first quarter revolution for all of Al, Cu and Fe. However, the revolution by 180° led to disappearance of the markers, indicating that slippage occurred during another 90° revolution. Although accurate estimation was not possible, the slippage was found to be as $0 < s < 1/2$ in this study.

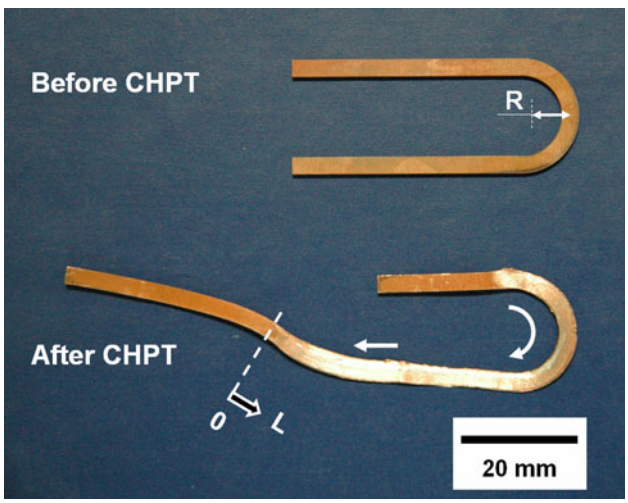

Fig. 2 Appearance of U-shaped Cu sample with $OD = 20$ mm before and after CHPT for 1 revolution

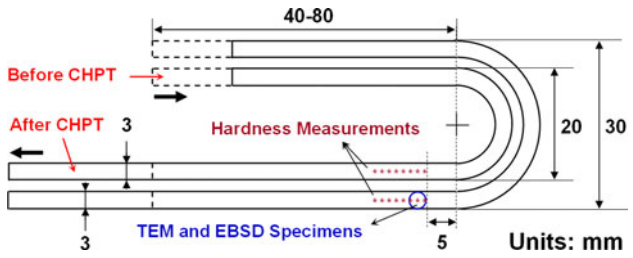

Fig. 3 Dimensions of U-shaped samples including positions for microhardness measurements and locations for EBSD and TEM disk

The experiments were conducted using high-purity Al (99.99%), Cu (99.99%), and Fe (99.96%) sheets, matching with those of the respective materials used in the earlier studies using conventional HPT [10–12]. The sheets were then cut to U-shaped specimens, as shown in Fig. 3, with 1-mm thickness, 3-mm width, and outer diameter of $OD = 20$ or 30 mm and 40–80 mm length. The Al and Cu specimens were annealed at 773 K and 873 K for 1 h, respectively. Each sample was placed on the lower anvil, and the upper and lower anvils were rotated with respect to each other at room temperature with a rotational speed of 1 rpm under a selected pressure of 1 GPa for Al, and 2 GPa for Cu and Fe. The rotation was terminated after 2 revolutions.

After completion of CHPT, the samples were subjected to Vickers microhardness measurement, and evaluated using electron back-scatter diffraction (EBSD) analysis and transmission electron microscopy (TEM).

First, both sides of the sample were polished to a mirror-like surface and the Vickers microhardness was measured at 16 points on upper and lower surfaces of the sample. Hardness was measured along the length in the center portion at every 1 mm starting from 5 mm away from the exit of the upper anvil, as shown by dotted lines in Fig. 3. The samples were further ground and polished mechanically, and the hardness was measured on the surface at the mid-point of thickness. For each hardness measurement, a load of 50 g for Al, and a load of 200 g for Cu and Fe were applied for 15 s, and the average of hardness values on the upper surface, lower surface, and the surface at the mid-point of thickness was calculated.

Second, disks with 3 mm in diameter were punched from the HPT disks at 5 mm away from the exit of the upper anvil as illustrated in Fig. 3. The 3-mm disks were ground mechanically to a thickness of 0.4 mm and further polished using an electro-chemical polisher using a solution of 10% $HClO_4$, 20% $C_3H_8O_3$ and 70% C_2H_5OH for Al, 15% HNO_3, 15% $C_3H_5(OH)_3$ and 70% CH_3OH for Cu, and 10% $HClO_4$ and 90% CH_3COOH for Fe. EBSD analysis was performed at a voltage of 20 kV, and the crystal orientations were determined using an automatic beam scanning system.

Third, for TEM, the 3-mm disk samples used for the EBSD analysis were ground mechanically to a thickness of 0.15 mm and further thinned with a twin-jet electro-chemical polisher using the solutions as mentioned above. TEM was performed at a voltage of 200 kV for micro-structural observation and for recording selected-area electron diffraction (SAED) patterns.

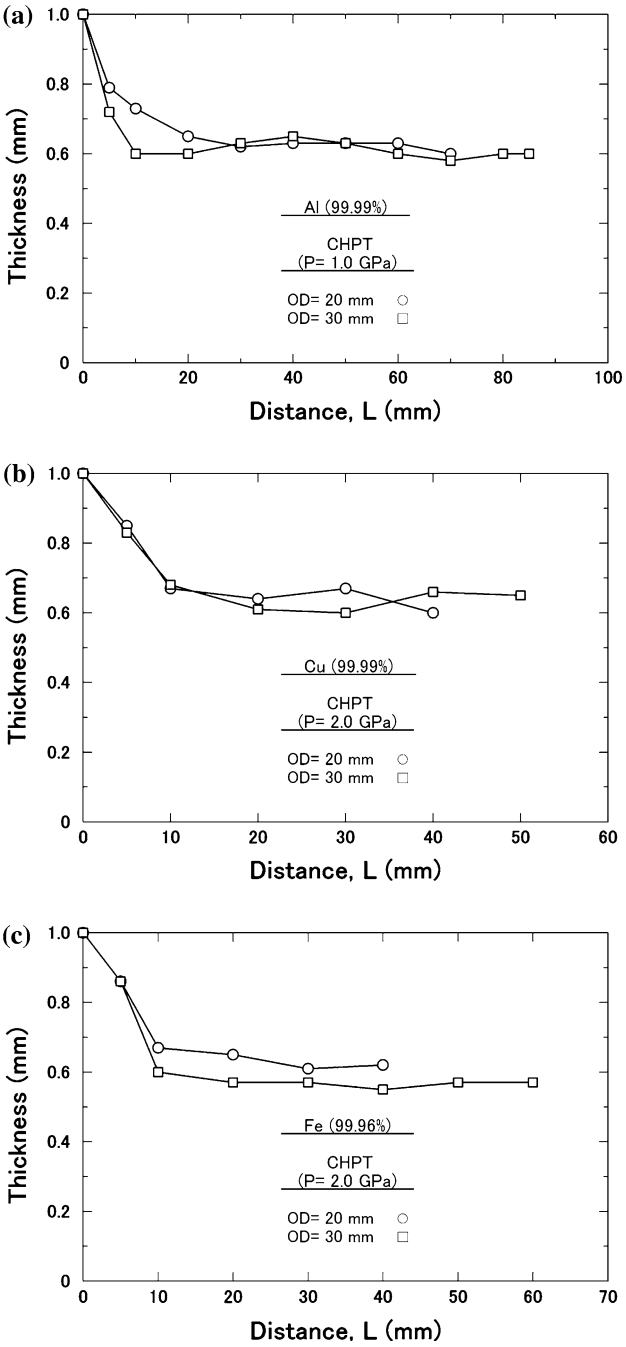

Fig. 4 Thickness variation along longitudinal direction of **a** Al, **b** Cu, and **c** Fe samples after CHPT

Results and discussion

Figure 4 shows the plots of the thickness variation against the distance, L, along the longitudinal direction for (a) Al, (b) Cu, and (c) Fe after processing with CHPT. The definition of L is shown in Fig. 2. The thickness is decreased from 1.0 to ~0.6 mm by CHPT, and it is almost uniform for $L > 10$ mm.

The hardness measured on the upper surface and the lower surface including the surface at the mid-point of thickness for samples with $OD = 20$ and 30 mm are given in Table 1. It is found that the hardness is reasonably the same on upper, middle, and lower surfaces, indicating a uniform microstructural evolution across the sample thickness. The average of hardness values among the upper, middle, and lower surfaces was taken for each sample and plotted in Fig. 5 together with earlier data obtained by conventional HPT of (a) Al, (b) Cu, and (c) Fe using disk and ring specimens [10–12]. There are two main points to be noted regarding the plots in Fig. 5: first, the results of HPT and CHPT are consistent, except that somewhat a higher value is obtained for Fe processed with CHPT; and second, the hardness values for CHPT-processed samples lie well on the steady-state (saturated) level obtained for disk samples and ring samples after processing with HPT. It should be noted that the present data were plotted using $s = 0$ in Eq. 1, and this may result in the overestimation of the equivalent strain. Nevertheless, the data points for Al, Cu, and Fe are still on the steady state levels.

An orientation image by EBSD is shown in Fig. 6a for Al after CHPT. TEM bright-field micrographs including SAED patterns are shown in Fig. 6b–d for Al, Cu, and Fe after CHPT, respectively. Inspection of Fig. 6a and b reveals that few dislocations are visible in the grains, and that grain boundaries are straight and well defined with an average grain size of ~2.1 μm in Al. These microstructural features are consistent with the earlier observations using conventional HPT, where an average grain size of ~1.9 μm was reported [15]. However, this value is higher than the grain sizes of ~1.2 μm reported previously for

Table 1 Hardness values on upper surface and lower surface including mid-point of thickness for Al, Cu, and Fe samples with $OD = 20$ and 30 mm after processing with CHPT

	Vickers microhardness (Hv)					
	$OD = 20$ mm			$OD = 30$ mm		
	Upper	Middle	Lower	Upper	Middle	Lower
Al (99.99%)	33	33	34	32	32	32
Cu (99.99%)	129	128	128	133	130	132
Fe (99.96%)	325	319	332	335	336	338

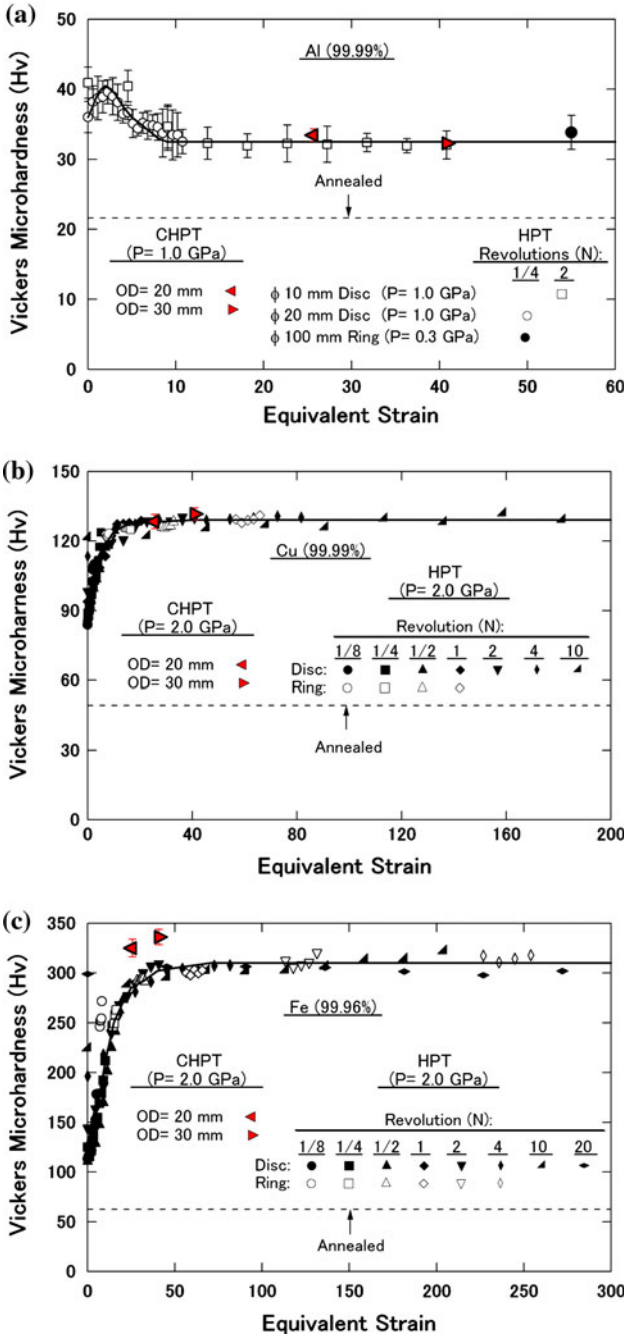

Fig. 5 Plots of Vickers microhardness against equivalent strain obtained earlier using conventional HPT for disk and ring specimens of **a** Al [12], **b** Cu [10], and **c** Fe [11] along with results of CHPT using U-shaped samples with $OD = 20$ and 30 mm

ECAP-processed samples [16, 17]. The difference in the grain size may be due to the difference between the microstructural evolutions occurring during HPT and ECAP. It is apparent from Fig. 6c and d that in Cu and Fe subjected to CHPT, the grain size is at submicrometer level with many ill-defined grain boundaries having high angles of misorientation as evidenced from the SAED patterns with well-defined rings. It was confirmed that most of

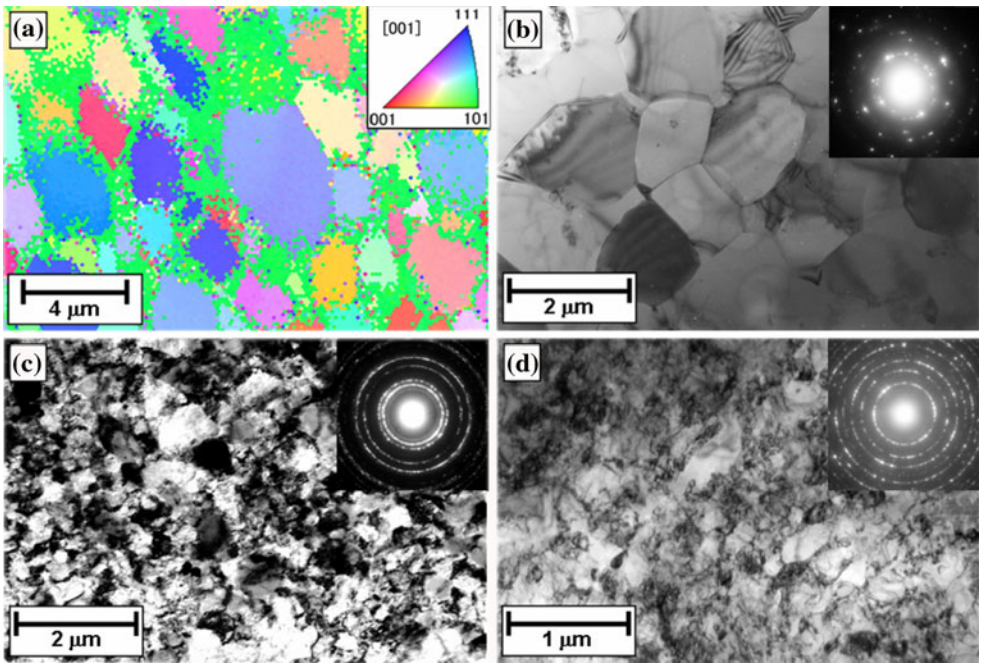

Fig. 6 **a** EBSD orientation image of Al; TEM micrographs and SAED patterns of **b** Al, **c** Cu, and **d** Fe after processing with CHPT

grains contain many dislocations but there are a few grains with a low density of dislocations. These microstructural features are also consistent with our earlier findings for HPT processing of Cu [10] and Fe [11].

In summary, it is emphasized that the method of CHPT can provide a continuous process for the conventional HPT while achieving grain refinement and subsequent strengthening in metallic materials without sacrificing the advantages of the conventional HPT. The method of CHPT has two main merits when compared to HPT and other SPD processing methods: first, a saturated level of hardness and a minimum grain size are reached in a short time and just after one pass through the anvils; second, CHPT can be used as a continuous process for producing metallic sheets and wires.

Summary and conclusions

A new severe plastic deformation process, called continuous high-pressure torsion (CHPT), was developed for microstructural refinement and subsequent enhancement of hardness. Sheets of high purity Al, Cu, and Fe with rectangular cross sections, 0.6-mm thickness and 3-mm width, were successfully processed by torsional straining under high pressure using CHPT.

Acknowledgements One of the authors (KE) thanks the Islamic Development Bank for a scholarship. This study was supported in part by the Light Metals Educational Foundation of Japan, in part by a Grant-in-Aid for Scientific Research from the Ministry of Education, Culture, Sports, Science, and Technology of Japan in the Priority Area "Giant Straining Process for Advanced Materials Containing Ultra-High Density Lattice Defects," and in part by Kyushu University Interdisciplinary Programs in Education and Projects in Research Development (P&P).

References

1. Valiev RZ, Islamgaliev RK, Alexandrov IV (2000) Prog Mater Sci 45:103
2. Valiev RZ, Estrin Y, Horita Z, Langdon TG, Zehetbauer MJ, Zhu YT (2006) JOM 58(4):33
3. Kolobov YR, Kieback B, Ivanov KV, Weissgaerber T, Girsova NV, Pochivalov YI, Grabovetskaya GP, Ivanov MB, Kazyhanov VU, Alexandrov IV (2003) Int J Refract Met Hard Mater 21:69
4. Wei Q, Zhang HT, Schuster BE, Ramesh KT, Valiev RZ, Kecskes LJ, Dowding RJ, Magness L, Cho K (2006) Acta Mater 54:4079
5. Rentenberger C, Waitz T, Karnthaler HP (2007) Mater Sci Eng A 462:283
6. Bridgman PW (1935) Phys Rev 48:825
7. Harai Y, Ito Y, Horita Z (2008) Scripta Mater 58:469
8. Erbel S (1979) Met Technol 6:482
9. Saunders I, Nutting J (1984) Metal Sci 18:571
10. Edalati K, Fujioka T, Horita Z (2008) Mater Sci Eng A 497:168
11. Edalati K, Fujioka T, Horita Z (2009) Mater Trans 50:44
12. Edalati K, Horita Z (2009) Mater Trans 50:92
13. Fujioka T, Horita Z (2009) Mater Trans 50:930
14. Edalati K, Horita Z, Langdon TG (2009) Scripta Mater 60:9
15. Edalati K, Ito Y, Suehiro K, Horita Z (2009) Int J Mater Res 100(12):1668
16. Iwahashi Y, Horita Z, Nemoto M, Langdon TG (1998) Acta Mater 46:3317
17. Kawasaki M, Horita Z, Langdon TG (2009) Mater Sci Eng A 524:143